

Particle yield fluctuations and chemical non-equilibrium at RHIC

Giorgio Torrieri

Department of Physics, McGill University, Montreal, QC H3A-2T8, Canada

Sangyong Jeon

*Department of Physics, McGill University, Montreal, QC H3A-2T8, Canada and
RIKEN-BNL Research Center, Upton NY, 11973, USA*

Johann Rafelski

*Department of Physics, University of Arizona, Tucson AZ 85721, USA and
CERN-PH-TH, 1211 Geneva 23, Switzerland*

(Dated: August 27, 2005)

We study particle yield fluctuations within the statistical hadronization model. Considering both the particle yield ratios and the yield fluctuations we show that it is possible to differentiate between chemical equilibrium and non-equilibrium freeze-out conditions. As an example of the procedure we show quantitatively how the relative yield ratio Λ/K^- together with the normalized net charge fluctuation $v(Q) = \langle \Delta Q^2 \rangle / \langle N_{\text{ch}} \rangle$ constrain the chemical conditions at freeze-out.

PACS numbers: 25.75.-q, 24.60.-k, 24.10.Pa

In relativistic heavy ion collisions a localized high energy density domain, a fireball, is created. The study of the properties of this hot and dense matter is the main objective of the experiments being conducted at RHIC and as of 2007 at LHC. Event-by-event particle fluctuations are the observables subject to intense current theoretical [1, 2, 3, 4, 5, 6, 7, 8, 9], and experimental interest [10, 11, 12]. Fluctuation measurements are important since they can be used: (i) as a consistency check for existing models, e.g. within statistical particle production models [2, 3], (ii) as a way to search for new physics, including QGP [4, 13, 14] (iii) as a test of particle equilibration [2, 9].

The statistical hadronization model (SHM), introduced by Fermi in 1950 [15, 16, 17], has been used extensively in recent years in the study of strongly interacting particle production. In this model, the properties of the final state particles are determined by requiring that the final state maximizes entropy given the physical properties of the fireball (energy, baryon content, etc.). When the full spectrum of hadronic resonances is included [18], the SHM turns into a quantitative model capable to describe in detail the abundances of all hadronic particles.

Fluctuations in conserved quantum numbers (such as charge, baryon number, strangeness, or equivalently the net number of valance up, down, strange quarks) can be studied only in the Grand Canonical (GC) ensemble, as in the micro and canonical ensembles these quantities are fixed. We recall that fluctuations of non-conserved observables, e.g. other hadron multiplicities, differ for different ensembles in the thermodynamic limit [19, 20]. It is important to remember that in particular near to a phase transition further sources of fluctuations can arise due to irreducible two particle correlations in such distributions. These effects go beyond the scope of this work.

A study of GC SHM fluctuations of conserved quantities is of considerable interest at RHIC. In view of detec-

tor coverage limitations we observe only a small portion of the fireball. Provided the fireball is indeed thermalized, the observable phase space window exchanges particles and energy with the unobserved much larger background “bath”, giving rise to fluctuations in conserved quantum numbers, in the same sense that the density of air molecules fluctuates locally even though their number is conserved (no particle production).

The situation is of particular interest for a reaction system at RHIC that exhibits a sizable rapidity plateau. It can be shown [21] that observables in a window around mid-rapidity (denoted as b.i. for boost-invariant) could be related to a static GC system with the same temperature and chemical potentials.

$$\frac{\langle N_i \rangle_{\text{GC}}}{\langle N_j \rangle_{\text{GC}}} = \frac{(dN_i/dy)_{\text{b.i.}}}{(dN_j/dy)_{\text{b.i.}}} \quad (1)$$

The derivation in [21] can also be applied to fluctuations

$$\frac{\langle \Delta N_i^2 \rangle_{\text{GC}}}{\langle N_j \rangle_{\text{GC}}} = \frac{(d \langle \Delta N_i^2 \rangle / dy)_{\text{b.i.}}}{(dN_j/dy)_{\text{b.i.}}} \quad (2)$$

Where we denote the variance (fluctuation) of any quantity X as $\langle \Delta X^2 \rangle = \langle X^2 \rangle - \langle X \rangle^2$. Given this, SHM yield fluctuations can be calculated by a textbook method, as are the average particle yields, as follows.

For a hadron with an energy $E_p = \sqrt{p^2 + m^2}$, the single particle occupancy factor for an energy level is given by:

$$n_i(E_p) = \frac{1}{\lambda_i^{-1} e^{E_p \beta} \pm 1}, \quad (3)$$

where the upper sign is for Fermions and the lower sign is for Bosons. Here λ_i is the particle fugacity, related to particle chemical potential $\mu_i = T \ln \lambda_i$.

The yield average and fluctuation is then given by:

$$\langle N_i \rangle = gV \int \frac{d^3 p}{(2\pi)^3} n_i(E_p), \quad (4)$$

$$\langle \Delta N_i^2 \rangle = gV \int \frac{d^3 p}{(2\pi)^3} n_i(E_p) (1 \mp n_i(E_p)). \quad (5)$$

When studying finite systems the consideration of fluctuations in *extensive* quantities such as of particle yield has to address also volume fluctuations when the volume cannot be fixed by boundary conditions. In our case volume fluctuations can arise due to initial reaction effects, impact parameter variations, as well as from fluctuation due to dynamics of the expansion of the fireball. It is difficult to arrive at a reliable description of all these effects. Therefore it is important to select fluctuation observables in which volume fluctuation effects are sub-dominant. Among extensive quantities, the net charge fluctuation stands out as it is relatively easy to measure and can be shown to be nearly independent of the volume fluctuations [1].

In light of the above considerations we concentrate our effort on the following net charge fluctuation measure:

$$v(Q) \equiv \langle \Delta Q^2 \rangle / \langle N_{\text{ch}} \rangle \quad (6)$$

proposed in the past as a probe of the QGP formation [4]. First results for $v(Q)$ are also available from RHIC experiments [11, 12].

The charged particle multiplicity is given by summing all final state (stable) charged particle multiplicities. These can be computed by adding the direct yield and all resonance decay feed-downs. The total yield of a stable particle α is

$$\langle N_\alpha \rangle_{\text{total}} = \langle N_\alpha \rangle + \sum_{j \neq \alpha} B_{j \rightarrow \alpha} \langle N_j \rangle. \quad (7)$$

where j labels resonances. $B_{j \rightarrow \alpha}$ is the probability (branching ratio) for the decay products of j to include α . The charged particle multiplicity is given by the sum of all charged stable particles.

The net charge fluctuations is given by

$$\langle \Delta Q^2 \rangle = \sum_i q_i^2 \langle \Delta N_i^2 \rangle \quad (8)$$

where q_i is charge density and i labels either *all* particles *before* resonance decays or *stable* particles *after* resonance decays, since decays conserve net charge [3]. To use Eq.(8), however, the experimental rapidity window must be large enough to encompass all decay particles of the resonances. Hence, our analysis applies to detectors which have a reasonable rapidity coverage, as well as full azimuthal acceptance (the latter also eliminates fluctuations resulting from differing reaction plane orientations (non-zero v_2) which would appear in multiplicity fluctuations in detectors with partial azimuthal coverage). Detectors such as STAR and NA49 are therefore optimally configured to perform such a measurement.

In a scenario where freeze-out occurs as a break-up of a *chemically equilibrated* hadron gas, detailed balance demands that for the hadron i the fugacity is given by the product of the fugacities of conserved quantum numbers.

$$\lambda_i^{\text{eq}} = \lambda_q^{q-\bar{q}} \lambda_s^{s-\bar{s}} \lambda_{I_3}^{I_3}, \quad \lambda_i^{\text{eq}} = (\lambda_i^{\text{eq}})^{-1}, \quad (9)$$

where \bar{q}, q is the number of light anti-quarks and quarks, respectively and \bar{s}, s is the number of strange anti-quarks and quarks, respectively and I_3 is the isospin. This formula implies that the fugacity for the antiparticle is, in full chemical equilibrium, the inverse of the fugacity for the particle, and the fugacity for a hadron carrying vanishing conserved quantum numbers is 1.

In our approach, we do not assume that that the chemical equilibrium is reached [22, 23]. Hence Eq.(9) no longer applies. The deviation from detailed balance can be parametrized by a phase space occupancy factor γ_q (for u, \bar{u}, d, \bar{d} in hadrons) and γ_s (for s and \bar{s}). In this *chemical nonequilibrium* case the fugacity becomes

$$\lambda_i = \lambda_i^{\text{eq}} \gamma_q^{q+\bar{q}} \gamma_s^{s+\bar{s}} \quad (10)$$

where λ_i^{eq} is given by Eq.(9) (Note that $\gamma_i = \gamma_{\bar{i}}$).

Chemical nonequilibrium is of a particular interest since it can result in a large pion fugacity which influences fluctuations much more severely than the yields. Light quark chemical nonequilibrium is well motivated in a scenario where an entropy rich deconfined state quickly hadronizes [24]. In this scenario, mismatch of entropies between the two phases requires $\gamma_q > 1$. If γ_q becomes large enough so that λ_π approaches $e^{m_\pi/T}$, then the pion yield and the fluctuations behave like (c.f. Eqs.(4,5))

$$\lim_{\epsilon \rightarrow 0} \langle N \rangle \propto \epsilon^{-1}, \quad \lim_{\epsilon \rightarrow 0} \langle \Delta N \rangle^2 \propto \epsilon^{-2}. \quad (11)$$

where $\epsilon = 1 - \lambda_\pi e^{-m_\pi/T}$. The fluctuation grows much faster than the yield as mentioned above.

Some studies of yield ratios have indeed found the value of γ_q that can potentially make ϵ small [23, 25, 26, 27]. However, other studies of yield ratios [28] concluded that γ_q is not necessarily large due to the fact parameters in such fits are highly correlated. In this case, adjusting other parameters such as the temperature can easily accommodate current data without having $\gamma_q > 1$. Since such conflict is common when only the *yields* are considered, it becomes necessary to study fluctuations as an additional constraint to determine the occupation factor γ_q more convincingly.

We now discuss our specific results. We use the public domain SHM suite of programs SHARE [29] to calculate yields and fluctuations, allowing for production of hadron resonances, their decay, and a possible absence of chemical equilibrium. In the rest of this paper, we set $\lambda_{I_3}^{\text{eq}} = 1$, $\lambda_q^{\text{eq}} = e^{\mu_B/3T} = 1.05$ and $\lambda_s^{\text{eq}} = 1.027$ in accordance with [26]. However, both observables we consider, the net charge fluctuations and the Λ/K^- particle yield ratio, are nearly independent of these quantities as will be shown below.

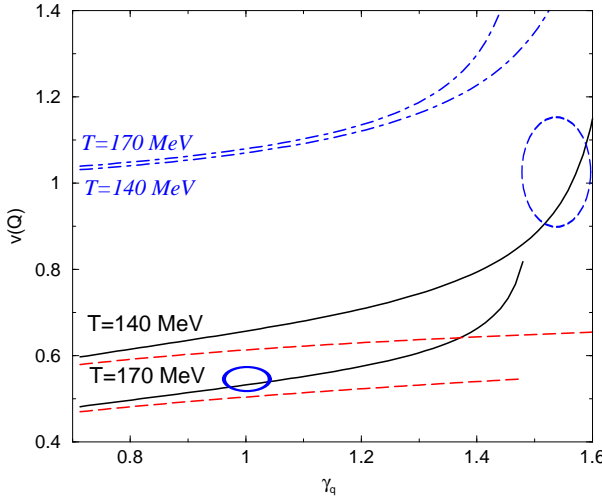


FIG. 1: $v(Q)$ as function of γ_q (solid lines). Dot-dashed lines, no resonance decays; dashed lines, Boltzmann fluctuations. Ellipses (blue) indicate the expected result areas for the equilibrium ($\gamma_q = 1$, solid) and non-equilibrium ($\gamma_q \neq 1$, dashed) models.

Fig. 1 shows the variation in $v(Q)$ as a function of γ_q for $T = 140, 170$ MeV. The solid lines show $v(Q)$ including the resonance decays, dot-dashed lines comprise only the direct effect of pion fluctuations. As the temperature increases (solid lines from top to bottom) the number of resonances increases. This in turn increases the unlike-sign charge correlations and hence reverses the temperature dependence of the pure pion case (dot-dashed lines). The short dashed lines show results for Boltzmann statistics. Boltzmann charge fluctuations are nearly constant as function of γ_q and primarily depend on chemical mix of the directly produced and secondary decay particles, which dominantly depend on the temperature T . The solid and dot-dashed lines in Fig. 1 terminate when the fluctuations start to diverge as in Eq.(11).

To determine both T and γ_q values we require an additional observable. In this work, we choose the yield ratio Λ/K^- . This ratio depends linearly on γ_q , and is nearly independent of λ_s^{eq} and γ_s as $\Lambda = (sdu)$ and $K^- = (s\bar{u})$. In Fig. 2 we show how the relative yield depends on γ_q and T . The Λ yield we wish to consider does not include weak decay feed from Ξ but it includes the electromagnetic decay of Σ^0 and the strong decays. K^- excludes feed-down from ϕ , but includes K^* and higher resonances. It is important to exclude the Ξ and ϕ cascading in order to eliminate the dependence on γ_s and λ_s^{eq} . Fortunately, this is experimentally feasible.

We now combine results in Figs. 1 and 2 into our main result Fig. 3. Every point in this plane of $v(Q)$ and Λ/K^- corresponds to a specific set of T and γ_q as indicated by the grid. Note that some domains in this plane are not allowed since they lie in the region where the (generating, GC) partition function cannot be defined. The two highlighted regions indicate the expected chemical

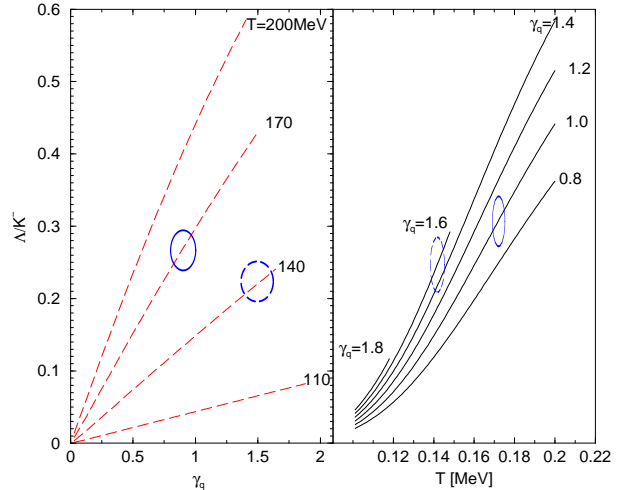


FIG. 2: Particle yield ratio Λ/K^- as a function of T and γ_q . The Λ yield does not include $\Xi \rightarrow \Lambda$ and the K^- yield is without the contribution of $\phi \rightarrow K^+K^-$ decays. Ellipses (blue) indicate the expected result areas for the equilibrium ($\gamma_q = 1$, solid) and non-equilibrium ($\gamma_q \neq 1$, dashed) models.

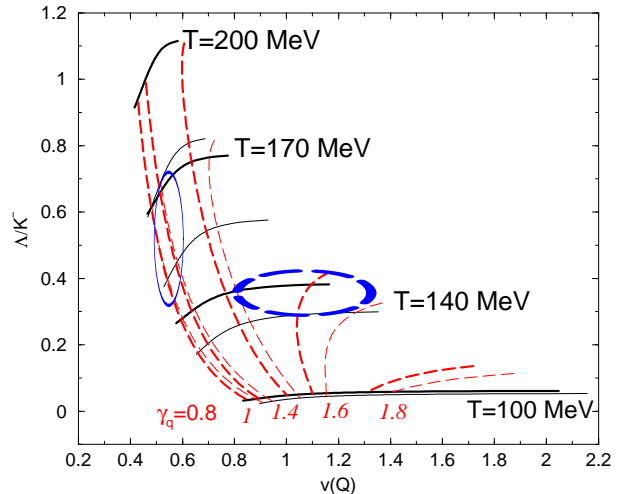


FIG. 3: Particle ratio Λ/K^- and particle fluctuation $v(Q)$ plane: a point in plane corresponds to a set of values γ_q, T . Lines correspond to results at fixed $T = 200$ (top), 170, 140, 100 MeV (bottom). The solid lines (black) are for $\gamma_q = 1$, dashed lines (red) for γ_q as indicated in the figure (from 0.7 on left to 1.8 to right). Thick lines correspond to $\gamma_s = 2.5$, thin lines correspond to $\gamma_s = 1$. Ellipses (blue) indicate the expected result areas for the equilibrium ($\gamma_q = 1$, solid) and non-equilibrium ($\gamma_q \neq 1$, dashed) models.

equilibrium (solid line ellipse at small $v(Q)$, corresponding to $\gamma_q = 1$ and $T = 170$ MeV) and nonequilibrium parameter domains (dashed line ellipse at larger $v(Q)$, corresponding to $\gamma_q = 1.62$ and $T = 140$ MeV). When particle yields and fluctuations are considered, the separation of these two domains confirms that we have found a sensitive method to determine both γ_q and T . The re-

sults of having two extreme values, $\gamma_s = 1$ and $\gamma_s = 2.5$, are also shown in Fig. 3. The γ_s values corresponds to the equilibrium [30] and non-equilibrium [23] best fits. Their difference, as seen in Fig. 3, is small and well below the experimental error. The largest remaining systematic deviation is due to the baryon chemical potential $e^{\mu_B/3T} = \lambda_q^{\text{eq}}$. It's contribution to $v(Q)$ is negligible, but this is not true for the case of Λ/K^- . Generally the value of λ_q^{eq} is well determined by baryon to antibaryon yield ratios in a model independent way.

To transform the diagram in Fig. 3 to an equivalent result applicable to lower reaction energy where λ_q^{eq} is greater, one has to allow for this change: We note that $\Lambda/K^- \propto (\lambda_q^{\text{eq}})^3$, and thus we need to multiply the axis in Figs. 2 and 3 by $(\lambda_q^{\text{eq}})^3/1.05^3$. One can actually use the Λ/K ratio in this. Since $\Lambda K^+/\bar{\Lambda} K^- \propto (\lambda_q^{\text{eq}})^6$, the axis rescaling would be done with $(\Lambda K^+/\bar{\Lambda} K^-)^{1/2}/1.05^3$ (Λ, K corrected for Ξ and ϕ feed-down).

One can ask whether γ_q and T as defined by results shown in Fig. 3 in turn imply that the SHM is a valid physical model. We required that the experimental results on yields and fluctuations are described by the same values of γ_q and T . This means that we fit the first and second derivative of the statistical GC-SHM partition function to the experimental data. We also are able to describe precisely other than here considered particle yields, also as function of impact parameter [26]. A study of reaction energy dependence [27] provides further sup-

port for the SHM. Further work on fluctuation tests of SHM is progressing [31]. Contrary to popular view the use of SHM does not require that there is an actual interacting phase of hadrons present. In a sudden breakup of the deconfined QGP into freely out-streaming hadrons the GC-SHM partition function is a generating function for the resulting particle production phase space [22, 23].

We have argued in this work that a simultaneous measurement of charge fluctuations and Λ/K^- ratios can differentiate between chemical equilibrium and non-equilibrium freeze-out, and to constrain the magnitude of the deviation from equilibrium. It is possible to distinguish the chemical equilibrium freeze-out condition $\gamma_q = 1$ ($T = 140-150$ MeV [26] or 170 MeV [30]) from the chemical non-equilibrium freeze-out condition $\gamma_q = 1.6, T = 140 \pm 4$ MeV [23, 26]. Hence an experimentally observed value of net charge fluctuations should be considered as a constraint when fitting the parameters in statistical hadronization models.

GT thanks C. Gale, L. Shi, V. Topor Pop and A. Bourque for helpful discussions and the Tomlinson foundation for support. S.J. thanks RIKEN BNL Center and U.S. Department of Energy [DE-AC02-98CH10886] for providing facilities essential for the completion of this work. Work supported in part by grants from the U.S. Department of Energy (J.R. by DE-FG02-04ER41318), the Natural Sciences and Engineering research council of Canada, the Fonds Nature et Technologies of Quebec.

[1] S. Jeon and V. Koch, "Event-by-event fluctuations," arXiv:hep-ph/0304012, In: Hwa, R.C. (ed.) et al.: *Quark gluon plasma*, Singapore 2004, pp 430-490.

[2] S. Jeon, V. Koch, K. Redlich and X. N. Wang, Nucl. Phys. A **697**, 546 (2002).

[3] S. Jeon and V. Koch, Phys. Rev. Lett. **83**, 5435 (1999).

[4] S. Jeon and V. Koch, Phys. Rev. Lett. **85**, 2076 (2000).

[5] M. Asakawa, U. W. Heinz and B. Muller, Phys. Rev. Lett. **85**, 2072 (2000).

[6] S. Mrowczynski, Phys. Rev. C **57**, 1518 (1998).

[7] C. Pruneau, S. Gavin and S. Voloshin, Phys. Rev. C **66**, 044904 (2002).

[8] J. Zaranek, Phys. Rev. C **66**, 024905 (2002)

[9] Q. H. Zhang, V. Topor Pop, S. Jeon and C. Gale, Phys. Rev. C **66**, 014909 (2002)

[10] J. G. Reid [STAR Collaboration], Nucl. Phys. A **698** (2002) 611.

[11] J. Adams *et al.* [STAR Collaboration], Phys. Rev. C **68**, 044905 (2003).

[12] K. Adcox *et al.* [PHENIX Collaboration], Phys. Rev. Lett. **89**, 082301 (2002).

[13] A. Bialas and R. C. Hwa, Phys. Lett. B **253**, 436 (1991).

[14] S. Hegyi and T. Csorgo, Phys. Lett. B **296**, 256 (1992).

[15] E. Fermi, Prog. Theor. Phys. **5**, 570 (1950).

[16] I. Pomeranchuk, Proc. USSR Academy of Sciences **43**, 889 (1951).

[17] L. D. Landau, Izv. Akad. Nauk Ser. Fiz. **17** (1953) 51.

[18] R. Hagedorn, Suppl. Nuovo Cimento **2**, 147 (1965).

[19] V. V. Begun, M. I. Gorenstein, A. P. Kostyuk and O. S. Zozulya, arXiv:nucl-th/0410044.

[20] V. V. Begun, M. Gazdzicki, M. I. Gorenstein and O. S. Zozulya, Phys. Rev. C **70**, 034901 (2004).

[21] J. Cleymans, K. Redlich, Phys. Rev. C **60**, 054908 (1999).

[22] J. Letessier and J. Rafelski, Cambridge Monogr. Part. Phys. Nucl. Phys. Cosmol. **18**, 1 (2002), see section 19.3.

[23] J. Rafelski, J. Letessier, Acta Phys. Polon. B **34**, 5791 (2003). J. Rafelski, J. Letessier, J. Phys. G **30**, S1 (2004).

[24] J. Rafelski and J. Letessier, Phys. Rev. Lett. **85**, 4695 (2000).

[25] J. Letessier and J. Rafelski, Int. J. Mod. Phys. E **9**, 107, (2000).

[26] J. Rafelski, J. Letessier, G. Torrieri, arXiv:nucl-th/0412072, Phys. Rev. C (2005) in press.

[27] J. Letessier and J. Rafelski, arXiv:nucl-th/0504028.

[28] F. Becattini, M. Gazdzicki, A. Keranen, J. Manninen and R. Stock, Phys. Rev. C **69**, 024905 (2004).

[29] G. Torrieri, W. Broniowski, W. Florkowski, J. Letessier, J. Rafelski, S. Steinke, Comp. Phys. Com. **167**, 229 (2005), see also: www.physics.arizona.edu/~torrieri/SHARE/share.html

[30] P. Braun-Munzinger, D. Magestro, K. Redlich and J. Stachel, Phys. Lett. B **518**, 41 (2001).

[31] G. Torrieri, S. Jeon, J. Rafelski, ISMD2005-Kromeriz, Aug. 9-15 2005. To appear shortly.